

Holographic Image Compression using New Biorthogonal Wavelets

N. Hyndavi¹, T. Aruna²

¹PG Scholar, Dept. of ECE, GKCE, Sullurpet

²Assistant Professor, Dept. of ECE, GKCE, Sullurpet

ABSTRACT

Digital holography refers to the acquisition and processing of holographs. Image rendering, or reconstruction of object data is performed numerically from digitized interferograms. Digital holography offers a means of measuring optical phase data and typically delivers three-dimensional surface or optical thickness images. Several recording and processing schemes have been developed to assess optical wave characteristics such as amplitude, phase, and polarization state, which make digital holography a very powerful method for metrology applications. With the invent of wavelet based coding schemes like Embedded Zerotree Wavelet and Set Partitioning in Hierarchical Trees, the image compression and image processing community as a whole has taken a turn to the study of wavelet analysis. Defining a suitable wavelet involves the shape, size and also the number of the basis functions. The important features of basis functions are vanishing moments, size of support, regularity and etc. Towards this end in this research work, the features of basis functions will be explored to find an optimal mother wavelet to be used in digital holography. In this paper, biorthogonal wavelets are explored and new variations are built and proved that the performance is superior to many existing ones.

Keywords: Spline function, image compression, biorthogonal wavelet, basis functions, holographic images

I.INTRODUCTION

Consider wavelet transformation of an image for compression. Discrete wavelet transform will be applied to the image; the result of this transformation is wavelet coefficients or what is called wavelet domain. The transformation actually transforms the less correlated data to highly correlated data. When the inverse transform is applied directly on the transformed coefficients the original signal should be restored. Otherwise the transformation should not be used. This condition is called perfect reconstruction. All well-known wavelet transforms satisfy this condition [1][2].

In transform coding schemes like Embedded zero tree wavelet (EZW) or Set partitioning in hierarchical trees (SPIHT), the coding scheme will be applied on wavelet domain or wavelet coefficients. Actually these coding schemes are formulated based on the structure of wavelet decomposition (coefficients) only. After performing the coding of these coefficients in a systematic way (called encoding) the compressed data is obtained. Here whenever we want to view the image the decoding and then inverse wavelet transform is applied [3]. Then

spatial domain image (generally deteriorated) is obtained. The aim of compression is to get a close reconstructed image (with original image) using few wavelet coefficients (or very less amount of memory). But this is very tough to maintain two things at a time because fundamentally these are inversely related [4].

All well-known wavelets satisfy perfect reconstruction condition, i.e., when we apply inverse wavelet transform directly on wavelet domain of the image we get exact original image. But when coding is applied on the wavelet domain the reconstructed image is different from original image and also it is different for different wavelet bases. So, the error between original and reconstructed image and size of coded wavelet coefficients depends on the wavelet bases used [5][6]. The wavelet bases are characterized by using parameters like vanishing moments, compact support, regularity, etc. Also compared to the orthogonal wavelets the biorthogonal wavelet system is flexible with more design options. Hence in this research new biorthogonal bases will be designed with the optimal wavelet bases for image compression in mind.

II. DESIGN OF BIORTHOGONAL WAVELETS

The design of biorthogonal wavelet is concerned in generating two sets of functions with certain properties. The two sets are supposed to be used one in decomposition and other in reconstruction phase of wavelet transform [7].

$$\int \phi(t) \tilde{\phi}(t-k) dt = \delta_{k,0}$$

$$\sum_n h(n) \tilde{h}(n-2k) = \delta_{k,0}$$

(1)

i.e., $h(n)$ is orthogonal to even translates of itself. Here \tilde{h} is orthogonal to h . Now let the positioning of $\phi(t)$ and $\tilde{\phi}(t)$ is from N_1 to N_2 and \tilde{N}_1 to \tilde{N}_2 respectively. The positioning of the scaling function coefficients is very important. This decides the constraints on coefficients. Now consider the following positioning [8].

$$N_1 = 1, \quad N_2 = 5 \text{ and } \tilde{N}_1 = 0, \quad \tilde{N}_2 = 6$$

(2)

Many applications require symmetric scaling function coefficients. So let us put this constraint first. Hence,

$$\tilde{h}(0) = \tilde{h}(6), \tilde{h}(1) = \tilde{h}(5) \text{ and } \tilde{h}(2) = \tilde{h}(4)$$

(3)

Now apply the conditions on coefficients. The equation $\int \tilde{\phi}(t) dt = 1$ results

$$2\tilde{h}(0) + 2\tilde{h}(1) + 2\tilde{h}(2) + \tilde{h}(3) = \sqrt{2}$$

(4)

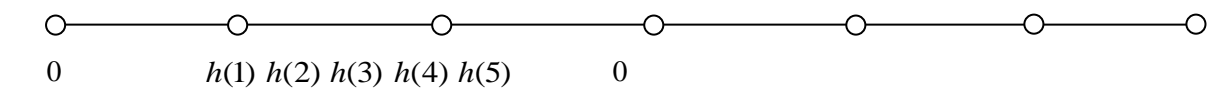
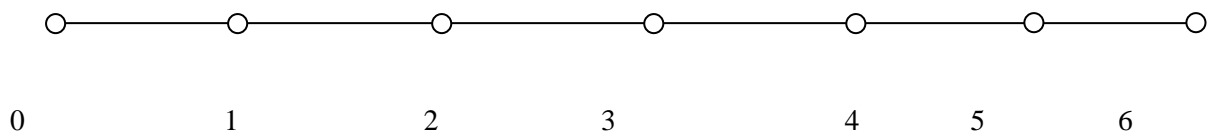
Now use equation (1), i.e.,

$$\sum_n h(n) \tilde{h}(n-2k) = \delta_{k,0}.$$

Substituting k = 0 in

$$\sum_n h(n) \tilde{h}(n-2k) = \delta_{k,0},$$

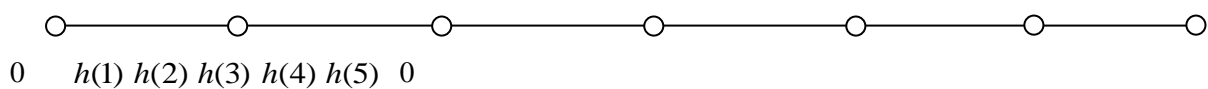
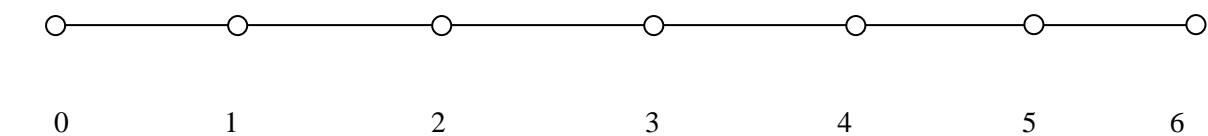
$$\tilde{h}(0) \tilde{h}(1) \tilde{h}(2) \tilde{h}(3) \tilde{h}(2) \tilde{h}(1) \tilde{h}(0)$$



$$h(1)\tilde{h}(1) + h(2)\tilde{h}(2) + h(3)\tilde{h}(3) + h(4)\tilde{h}(2) + h(5)\tilde{h}(1) = 1 \tag{5}$$

Substituting k = 1 in $\sum_n h(n) \tilde{h}(n-2k) = \delta_{k,0}$,

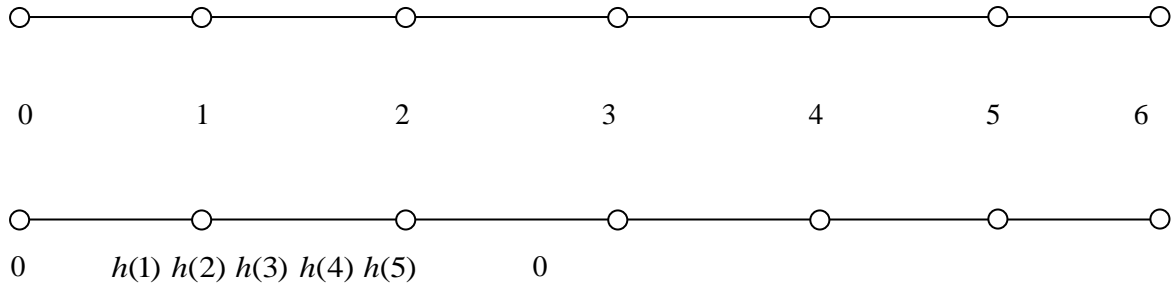
$$\tilde{h}(0) \tilde{h}(1) \tilde{h}(2) \tilde{h}(3) \tilde{h}(2)$$



$$h(2)\tilde{h}(0) + h(3)\tilde{h}(1) + h(4)\tilde{h}(2) + h(5)\tilde{h}(3) = 0 \tag{6}$$

Substituting k = 2 in $\sum_n h(n) \tilde{h}(n-2k) = \delta_{k,0}$,

$\tilde{h}(0) \tilde{h}(1) \tilde{h}(2)$



$$h(4)\tilde{h}(0) + h(5)\tilde{h}(1) = 0 \tag{7}$$

The general form of Spline of order k is given by

$$N_k(t) = \sum_{i=0}^k p_i N_k(2t - i)$$

Where $p_i = \frac{1}{2^{k-1}} \binom{k}{i}$

Consider Spline of order 4 which is given below.

$$N_4(t) = \frac{1}{8} N_4(2t) + \frac{4}{8} N_4(2t-1) + \frac{6}{8} N_4(2t-2) + \frac{4}{8} N_4(2t-3) + \frac{1}{8} N_4(2t-4)$$

The above spline is considered as one of the scaling function.

Hence the un-normalized coefficients becomes, $\frac{1}{8}, \frac{4}{8}, \frac{6}{8}, \frac{4}{8}$ and $\frac{1}{8}$.

The sum of normalized coefficients must be equal to $\sqrt{2}$ this follows from the requirement

$$\int \phi(t) dt = 1.$$

Therefore $a \left(\frac{1}{8} + \frac{4}{8} + \frac{6}{8} + \frac{4}{8} + \frac{1}{8} \right) = \sqrt{2}$

$$\Rightarrow a = \frac{1}{\sqrt{2}}$$

Hence the normalized coefficients of $\phi(t)$ are:

$$\frac{1}{8\sqrt{2}}, \frac{4}{8\sqrt{2}}, \frac{6}{8\sqrt{2}}, \frac{4}{8\sqrt{2}} \text{ and } \frac{1}{8\sqrt{2}}.$$

Using Eqn. (2), the scaling coefficients becomes

$$h(1) = \frac{1}{8\sqrt{2}}, h(2) = \frac{4}{8\sqrt{2}}, h(3) = \frac{6}{8\sqrt{2}}, h(4) = \frac{4}{8\sqrt{2}} \text{ and } h(5) = \frac{1}{8\sqrt{2}} \quad (8)$$

Rewriting the above equations using Eqn. (8) becomes

$$\text{Eqn. (4)} \rightarrow 2\tilde{h}(0) + 2\tilde{h}(1) + 2\tilde{h}(2) + \tilde{h}(3) = \sqrt{2} \quad (9)$$

$$\text{Eqn. (5)} \rightarrow \frac{1}{4\sqrt{2}}\tilde{h}(1) + \frac{1}{\sqrt{2}}\tilde{h}(2) + \frac{3}{4\sqrt{2}}\tilde{h}(3) = 1 \quad (10)$$

$$\text{Eqn. (6)} \rightarrow \frac{1}{2\sqrt{2}}\tilde{h}(0) + \frac{3}{4\sqrt{2}}\tilde{h}(1) + \frac{1}{2\sqrt{2}}\tilde{h}(2) + \frac{1}{8\sqrt{2}}\tilde{h}(3) = 0 \quad (11)$$

$$\text{Eqn. (7)} \rightarrow \frac{1}{2\sqrt{2}}\tilde{h}(0) + \frac{1}{8\sqrt{2}}\tilde{h}(1) = 0 \quad (12)$$

For a total of 4 variables, four equations are formed but in these equations only the equations (9), (10) and (12) are independent. Hence another equation is formed below using vanishing moments. From vanishing moments condition,

$$\tilde{h}(6) - \tilde{h}(5) + \tilde{h}(4) - \tilde{h}(3) + \tilde{h}(2) - \tilde{h}(1) + \tilde{h}(0) = 0$$

$$\text{which implies } 2\tilde{h}(0) - 2\tilde{h}(1) + 2\tilde{h}(2) - \tilde{h}(3) = 0 \quad (13)$$

Solving (9), (10), (12) and (13) yields

$$\tilde{h}(0) = \frac{3\sqrt{2}}{32}, \tilde{h}(1) = -\frac{3\sqrt{2}}{8}, \tilde{h}(2) = \frac{5\sqrt{2}}{32} \text{ and } \tilde{h}(3) = \frac{5\sqrt{2}}{4}.$$

By symmetry

$$\tilde{h}(4) = \frac{5\sqrt{2}}{32}, \tilde{h}(5) = -\frac{3\sqrt{2}}{8} \text{ and } \tilde{h}(6) = \frac{3\sqrt{2}}{32}.$$

Since $\tilde{\phi}(t) \perp \psi(t)$, $g(k) = (-1)^k \tilde{h}(N - k - 1)$. Therefore

$$g(-1) = -\frac{3\sqrt{2}}{32}, g(0) = -\frac{3\sqrt{2}}{8}, g(1) = -\frac{5\sqrt{2}}{32}, g(2) = \frac{5\sqrt{2}}{4}, g(3) = -\frac{5\sqrt{2}}{32}, g(4) = -\frac{3\sqrt{2}}{8} \text{ and } g(5) = -\frac{3\sqrt{2}}{32}.$$

Similarly using $\tilde{g}(k) = (-1)^k h(M - k - 1)$

$$\tilde{g}(0) = \frac{1}{8\sqrt{2}}, \tilde{g}(1) = -\frac{4}{8\sqrt{2}}, \tilde{g}(2) = \frac{6}{8\sqrt{2}}, g(3) = -\frac{4}{8\sqrt{2}}, \text{ and } g(4) = \frac{1}{8\sqrt{2}}.$$

The coefficients of newly designed biorthogonal wavelet are given in the table below.

Table 1. Wavelet and scaling function coefficients

K	-1	0	1	2	3	4	5	6
\tilde{h}		0.1326	-0.5303	0.2210	1.7678	0.2210	-0.5303	0.1326
\tilde{g}		0.0884	-0.3536	0.5303	-0.3536	0.0884		
h			0.0884	0.3536	0.5303	0.3536	0.0884	
g	-0.1326	-0.5303	-0.2210	1.7678	-0.2210	-0.5303	-0.1326	

The above wavelet is denoted by ‘biors23’ since if we take the reference as zero, the coefficients spreads from -2 to 2 and -3 to 3. Similarly two more wavelets using spline functions with different positioning are designed. These are ‘biors12’ and ‘biors34’ where the coefficients spreads from -1 to 1 and -2 to 2 and -3 to 3 and -4 to 4.

III. NEW BASIS FUNCTION BASED BIORTHOGONAL WAVELETS

The standard Spline function is defined as follows.

$$N_k(t) = \sum_{i=0}^k p_i N_k(2t - i)$$

where $p_i = \frac{1}{2^{k-1}} \binom{k}{i}$.

Here the p_i is the scaling value of dilated and translated spline function. The scaling value is directly proportional to binomial coefficients [9][10]. Hence symmetry is guaranteed. The coefficients are linearly distributed. Now a modified Spline is proposed. The new spline-like function is supposed to have symmetry but the coefficient values are modified to have more weight at center and gradually approaches standard spline function. The p_i is modified and given below.

For $i \leq (k/2)$, $p_i = \frac{i+1}{2^{k-1}} \binom{k}{i}$ and

for $i > (k/2)$, $p_i = \frac{k-i+1}{2^{k-1}} \binom{k}{i}$.

The coefficients of the standard Spline and proposed Spline-like functions are given in Fig. 1.

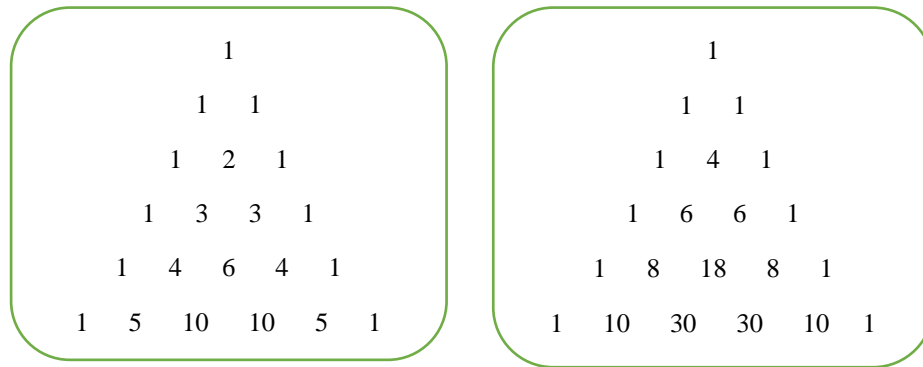


Figure 1. Coefficients of standard Spline function and proposed Spline-like function

In Fig.1, the coefficients are given by ignoring the division by 2^{k-1} . By using the above spline-like function with different lengths three wavelets are designed. These are denoted by ‘biorsl12’, ‘biorsl23’ and ‘biorsl34’ respectively. The spline-like functions of length 3, 5 and 7 are utilized for ‘biorsl12’, ‘biorsl23’ and ‘biorsl34’ respectively. The normalized coefficients of the spline-like function used for the wavelet ‘biorsl12’ ($k=2$) are given below.

$$h(-1) = p_0 = \frac{\sqrt{2}}{6}, \quad h(0) = p_1 = \frac{2\sqrt{2}}{3}, \quad h(1) = p_2 = \frac{\sqrt{2}}{6}$$

Similarly the coefficients for ‘biorsl23’ ($k=4$) and ‘biorsl34’ ($k=6$) are given below.

$$h(-2) = p_0 = \frac{2\sqrt{2}}{72}, \quad h(-1) = p_1 = \frac{2\sqrt{2}}{9}, \quad h(0) = p_2 = \frac{\sqrt{2}}{2}, \quad h(1) = p_3 = \frac{2\sqrt{2}}{9}, \quad h(2) = p_4 = \frac{2\sqrt{2}}{72}.$$

$$h(-3) = p_0 = \frac{\sqrt{2}}{196}, \quad h(-2) = p_1 = \frac{3\sqrt{2}}{49}, \quad h(-1) = p_2 = \frac{45\sqrt{2}}{196}, \quad h(0) = p_3 = \frac{20\sqrt{2}}{49},$$

$$h(1) = p_4 = \frac{45\sqrt{2}}{196}, \quad h(2) = p_5 = \frac{3\sqrt{2}}{49}, \quad h(3) = p_6 = \frac{\sqrt{2}}{196}$$

Using the property of double shift biorthogonality, normality, symmetry and vanishing moments the following equations are derived for ‘biorsl1’.

$$2\tilde{h}(-2) + 2\tilde{h}(-1) + \tilde{h}(0) = \sqrt{2}$$

$$2\tilde{h}(-2) - 2\tilde{h}(-1) + \tilde{h}(0) = 0$$

$$\tilde{h}(-1) + 2\tilde{h}(0) = 3/\sqrt{2}$$

$$\tilde{h}(-1) + 4\tilde{h}(-2) = 0$$

The unique solution to the above system of equations is given below.

$$\tilde{h}(-2) = -\frac{\sqrt{2}}{16}, \tilde{h}(-1) = \frac{\sqrt{2}}{4}, \tilde{h}(0) = \frac{5\sqrt{2}}{8}, \tilde{h}(1) = \frac{\sqrt{2}}{4}, \tilde{h}(2) = -\frac{\sqrt{2}}{16}.$$

Similarly the coefficients for ‘biors1’ and ‘biors2’ are calculated and the coefficients of ‘coifs2’ are given below.

$$\tilde{h}(-3) = -\frac{5\sqrt{2}}{256}, \tilde{h}(-2) = -\frac{5\sqrt{2}}{32}, \tilde{h}(-1) = \frac{59\sqrt{2}}{256}, \tilde{h}(0) = \frac{13\sqrt{2}}{16},$$

$$\tilde{h}(1) = \frac{59\sqrt{2}}{256}, \tilde{h}(2) = -\frac{5\sqrt{2}}{32}, \tilde{h}(3) = -\frac{5\sqrt{2}}{256}$$

The coefficients of ‘coifsl34’ are given below.

$$\tilde{h}(-4) = -\frac{\sqrt{2}}{128}, \tilde{h}(-3) = \frac{3\sqrt{2}}{32}, \tilde{h}(-2) = -\frac{5\sqrt{2}}{16}, \tilde{h}(-1) = \frac{5\sqrt{2}}{32}, \tilde{h}(0) = \frac{73\sqrt{2}}{64},$$

$$\tilde{h}(1) = \frac{5\sqrt{2}}{32}, \tilde{h}(2) = -\frac{5\sqrt{2}}{16}, \tilde{h}(3) = \frac{3\sqrt{2}}{32}, \tilde{h}(4) = -\frac{\sqrt{2}}{128}.$$

The above are scaling function coefficients at decomposition and reconstruction side. The wavelet function coefficients are calculated from these values using expressions presented in previous sections.

III.SIMULATION RESULTS

This section is concerned with the simulation results of proposed wavelets used in image compression. The image compression schemes considered are EZW [11], SPIHT [12]-[15], spatial oriented tree (STW), Wavelet difference reduction (WDR) and adaptively selected wavelet difference reduction schemes (ASWDR). The test images considered are holographic images. The simulation was carried on large number of holographic images, and results on 6 images are presented in this section. Compression ratio (CR), Peak signal to noise ratio (PSNR) and Structural similarity (SSIM) are evaluated. These values are given in Tables 2 to 6, each using different coding scheme.

Table 2. Compression results with EZW

Image	Parameter	BIORS – 1	BIORS - 2	NBIOR - 1	NBIOR – 2
1	CR	5.57	3.86	9.97	7.19
	PSNR	26.95	19.76	28.74	22.40
	SSIM	0.93	0.76	0.95	0.83
2	CR	11.90	2.82	22.75	16.19
	PSNR	29.15	15.77	33.24	27.24

	SSIM	0.92	0.44	0.95	0.83
3	CR	9.47	13.45	20.71	11.07
	PSNR	22.37	18.18	26.29	20.22
	SSIM	0.79	0.59	0.90	0.66
4	CR	6.58	5.43	12.70	8.26
	PSNR	31.06	23.97	33.66	28.26
	SSIM	0.88	0.65	0.91	0.77
5	CR	7.94	1.39	13.55	17.73
	PSNR	38.08	20.17	41.58	39.91
	SSIM	0.97	0.55	0.98	0.96
6	CR	26.42	4.45	37.62	47.15
	PSNR	47.34	26.42	49.50	44.95
	SSIM	0.99	0.51	0.99	0.97

Table 3. Compression results with SPIHT

Image	Parameter	BIORS - 1	BIORS - 2	NBIOR - 1	NBIOR - 2
1	CR	3.6087	2.4404	3.2873	4.7567
	PSNR	26.1213	19.0541	24.1373	21.7224
	SSIM	0.92216	0.73768	0.88011	0.80482
2	CR	7.9386	1.7466	7.9539	10.643
	PSNR	28.3256	15.5077	27.6953	26.2684
	SSIM	0.9102	0.41597	0.88143	0.80803
3	CR	6.7296	5.2261	5.6112	8.3216
	PSNR	22.0015	15.1597	21.1496	19.8948
	SSIM	0.77251	0.40269	0.71882	0.63342
4	CR	4.5664	1.9557	4.0095	5.5267
	PSNR	30.502	20.2151	29.4054	27.5773
	SSIM	0.87192	0.48083	0.82902	0.74209
5	CR	5.013	0.49591	8.6217	10.9985
	PSNR	37.1212	16.9451	40.3732	38.6803
	SSIM	0.96775	0.40436	0.97251	0.95226
6	CR	11.7966	1.624	17.9693	21.9955

	PSNR	41.5796	23.7292	45.6326	43.0904
	SSIM	0.96395	0.39073	0.97201	0.94831

Table 4. Compression results with STW

Image	Parameter	BIORS - 1	BIORS - 2	NBIOR - 1	NBIOR - 2
1	CR	5.1325	3.539	4.5776	6.7078
	PSNR	27.019	19.7979	25.0451	22.4944
	SSIM	0.93389	0.76529	0.89598	0.82735
2	CR	11.8474	2.5152	11.9654	16.0436
	PSNR	29.2839	15.7668	28.8566	27.5245
	SSIM	0.92252	0.43953	0.89834	0.83928
3	CR	9.785	7.7449	7.9707	11.6272
	PSNR	22.4244	15.4869	21.6035	20.2766
	SSIM	0.79177	0.4317	0.74118	0.65956
4	CR	6.4997	2.8392	5.5842	7.7993
	PSNR	31.1967	20.6166	30.3031	28.6499
	SSIM	0.8825	0.51031	0.84624	0.77924
5	CR	7.4443	0.68715	13.3372	17.249
	PSNR	38.4664	17.1371	43.1523	42.296
	SSIM	0.97358	0.41315	0.98101	0.97146
6	CR	17.3925	2.3371	26.6846	33.9111
	PSNR	43.9615	24.0129	50.1329	48.9213
	SSIM	0.97599	0.42525	0.98848	0.98061

Table 5. Compression results with WDR

Image	Parameter	BIORS - 1	BIORS - 2	NBIOR - 1	NBIOR - 2
1	CR	5.6824	4.0548	10.6979	7.7103
	PSNR	26.954	19.7575	28.7433	22.4007
	SSIM	0.93311	0.76418	0.95089	0.8251
2	CR	13.5417	2.9231	26.5121	19.042
	PSNR	29.1492	15.7688	33.2401	27.2354
	SSIM	0.92086	0.43959	0.9479	0.83108
3	CR	10.5509	14.7349	24.4863	13.1343

	PSNR	22.3746	18.1767	26.2868	20.2228
	SSIM	0.78952	0.58852	0.89718	0.65623
4	CR	7.1452	5.7958	14.0335	9.1283
	PSNR	31.0639	23.9727	33.6597	28.2584
	SSIM	0.87954	0.64747	0.91447	0.7697
5	CR	9.0083	1.413	16.2094	21.4671
	PSNR	38.0803	20.1726	41.5846	39.9106
	SSIM	0.97231	0.54858	0.97712	0.96322
6	CR	28.3427	4.6178	40.7277	52.3137
	PSNR	47.3422	26.4183	49.5037	44.9486
	SSIM	0.98946	0.50767	0.99114	0.97426

Table 6. Compression results with ASWDR

Image	Parameter	BIORS - 1	BIORS - 2	NBIOR - 1	NBIOR - 2
1	CR	5.5934	3.9708	10.5164	7.6538
	PSNR	26.954	19.7575	28.7433	22.4007
	SSIM	0.93311	0.76418	0.95089	0.8251
2	CR	13.2884	2.887	25.8657	18.7602
	PSNR	29.1492	15.7688	33.2401	27.2354
	SSIM	0.92086	0.43959	0.9479	0.83108
3	CR	10.4401	14.3611	24.0875	13.1195
	PSNR	22.3746	18.1767	26.2868	20.2228
	SSIM	0.78952	0.58852	0.89718	0.65623
4	CR	7.1025	5.6524	13.9277	9.1537
	PSNR	31.0639	23.9727	33.6597	28.2584
	SSIM	0.87954	0.64747	0.91447	0.7697
5	CR	8.5012	1.357	15.4043	20.3359
	PSNR	38.0803	20.1726	41.5846	39.9106
	SSIM	0.97231	0.54858	0.97712	0.96322
6	CR	27.1311	4.4769	39.0961	50.2151
	PSNR	47.3422	26.4183	49.5037	44.9486
	SSIM	0.98946	0.50767	0.99114	0.97426

IV.CONCLUSIONS

In this paper, new biorthogonal wavelets are proposed. The newly designed wavelets are used for image compression. Five different wavelet based image compression techniques are considered. They are EZW, SPIHT, STW, WDR, and ASWDR. Simulations are performed on Holographic images. The main observation from the simulation results is that the compression ratio using proposed wavelets is extremely high in comparison with that of in existing wavelets. In most of the cases the compression ratio using proposed wavelets is more than twice that of the existing wavelets. In addition to achieving high compression ratio a tolerable PSNR was maintain. The spline function when changed by considering a criterion and also when the input images classified based on their characteristics, a more generalized and optimum mother wavelet function can be devised with the analysis present in this paper.

REFERENCES

- [1] Ronald A. DeVore, "Adaptive Wavelet Bases for Image Compression", A K Peters Wavelets, Images and Surface Fitting, pp. 197-219, 1994.
- [2] Yan Zhuang, John S. Baras, "Image compression using optimal wavelet basis", Proc. of SPIE, 17-21 April 1995.
- [3] Michael G. Strintzis, "Optimal Biorthogonal Wavelet Bases for Signal Decomposition", IEEE Transactions on Signal Processing, vol. 44, no. 6, pp. 1406-1417, June 1996.
- [4] Aleksandra Mojsilovic, Miodrag V. Popovic and Dejan M. Rackov, "On the Selection of an Optimal Wavelet Basis for Texture Characterization", IEEE Transactions on Image Processing, vol. 9, no. 12, pp. 2043-2050, Dec 2000.
- [5] Nasir M. Rajpoot, Roland G. Wilson, Francois G. Meyer, Ronald R. Coifman, "Adaptive Wavelet Packet Basis Selection for Zerotree Image Coding", IEEE Transactions on Image Processing, vol. 12, no. 12, Dec 2003.
- [6] M. K. Mandal, S. Panchanathan and T. Aboulnasr, "Choice of Wavelets for Image Compression", Springer Lecture Notes in Computer Science, vol. 1133, pp. 239-249, 2005.
- [7] G. K. Kharate, V. H. Patil and N. L. Bhale, "Selection of mother wavelet for image compression on basis of image", Journal of Multimedia, vol. 2, no. 6, November 2007.
- [8] Maria Rehman, Imran Touqir, Wajiha Batool, "Selection of optimal wavelet bases for image compression using SPIHT algorithm", Proc. SPIE 9445, Seventh International Conference on Machine Vision (ICMV 2014), vol. 9445, Feb 2015.
- [9] Noor Kamal Al-Qazzaz, Sawal Hamid Bin Mohd Ali, Siti Anom Ahmad, Mohd Shabiul Islam and Javier Escudero, "Selection of Mother Wavelet Functions for Multi-Channel EEG Signal Analysis during a Working Memory Task", Sensors, 15, pp. 29015-29035, 2015.
- [10] Girisha Garg, "A signal invariant wavelet function selection algorithm", Springer Medical & Biological Engineering Computing, 54, pp. 629-642, 2016.

- [11] Shapiro J.M. (1993), "Embedded image coding using zerotrees of wavelet coefficients", *P IEEE Trans. Signal Proc.*, Vol. 41, No. 12, pp. 3445–3462.
- [12] Said A., W.A. Pearlman (1996), "A new, fast, and efficient image codec based on set partitioning in hierarchical trees," *IEEE Trans. on Circuits and Systems for Video Technology*, Vol. 6, No. 3, pp. 243–250.
- [13] Jaya Krishna Sunkara, PurnimaKuruma, Ravi Sankaraiah Y, "Image Compression Using HandDesigned and Lifting Based Wavelet Transforms", *International Journal of Electronics Communications and Computer Technology* (e-ISSN: 2249-7838, IF: 1.2456), Vol. 2 (4),2012.
- [14] Jaya Krishna Sunkara, E Navaneethasagari, D Pradeep, E Naga Chaithanya, D Pavani, D V SaiSudheer, "ANewVideoCompressionMethodusingDCT/DWTandSPIHTbasedonAccordionRepresentation", *I.J. Image, Graphics and Signal Processing* (e-ISSN: 2074-9082, p-ISSN:2074-9074,IF: 0.11), pp. 28-34, May2012.
- [15] JayaKrishnaSunkara,KurumaPurnima,ENavaneethaSagariandLRamaSubbareddy, "ANewAccordion Based Video Compression Method", *i-manager's Journal on Electronics Engineering*(e-ISSN: 2249-0760, p-ISSN: 2229-7286), Vol. 1, No. 4, pp. 14-21, June - August2011.

Author's Profile



N. Hyndavi, received her Bachelors in Technology in Electronics and Communication Engineering from Priyadarshini College of Engineering, Sullurpet affiliated to JNTUA, Ananthapuramu in 2015. Currently she pursuing Masters in Technology in Digital Electronics and Communication Systems in Gokula Krishna College of Engineering, Sullurpet. Her research interests include Signal and Image Processing and wavelet analysis.



Sullurpet.

T. Aruna, received her B.Tech degree in ECE from Audisankara College of Engineering and Technology, JNTU Hyderabad in 2005, M.Tech degree from Sri VenkataPerumala College of Engineering and Technology, JNTUA Ananthapuramu in 2012. Presently she is working as an Assistant Professor in the Department of ECE at Gokula Krishna College of Engineering,